Fungal Genetics and Biology 48 (2011) 1096–1107

Contents lists available at SciVerse ScienceDirect

Fungal Genetics and Biology

journal homepage: www.elsevier.com/locate/yfgbi

Novel Fusarium head blight pathogens from Nepal and Louisiana revealed by multilocus genealogical concordance

Brice A.J. Sarver [a], Todd J. Ward [b], Liane R. Gale [c], Karen Broz [d], H. Corby Kistler [c,d], Takayuki Aoki [e], Paul Nicholson [f], Jon Carter [f], Kerry O'Donnell [b,*]

[a] Department of Biological Sciences, University of Idaho, Moscow, ID 83844, USA
[b] Bacterial Foodborne Pathogens and Mycology Research Unit, National Center for Agricultural Utilization Research, Agricultural Research Service, United States Department of Agriculture, 1815 North University Street, Peoria, IL 61604-3999, USA
[c] Department of Plant Pathology, University of Minnesota, St. Paul, MN 55108, USA
[d] Cereal Disease Laboratory, US Department of Agriculture, Agricultural Research Service, 1551 Lindig Street, St. Paul, MN 55108, USA
[e] NIAS Genebank-Microorganisms Section (MAFF), National Institute of Agrobiological Sciences (NIAS), 2-1-2 Kannondai, Tsukuba, Ibaraki 305-8602, Japan
[f] Department of Disease and Stress Biology, John Innes Centre, Norwich Research Park, Colney Lane, Norwich NR4 7UH, UK

ARTICLE INFO

Article history:
Received 10 June 2011
Accepted 23 September 2011
Available online 7 October 2011

Keywords:
Deoxynivalenol
15ADON
Fusarium head blight
Genealogical concordance
Mycotoxin
Nivalenol
Phylogeny
Reciprocal monophyly
Trichothecene

ABSTRACT

This study was conducted to assess evolutionary relationships, species diversity and trichothecene toxin potential of five *Fusarium graminearum* complex (FGSC) isolates identified as genetically novel during prior Fusarium head blight (FHB) surveys in Nepal and Louisiana. Results of a multilocus genotyping (MLGT) assay for B-trichothecene species determination indicated these isolates might represent novel species within the FGSC. GCPSR-based phylogenetic analyses of a 12-gene dataset, comprising portions of seven loci totaling 13.1 kb of aligned DNA sequence data, provided strong support for the genealogical exclusivity of the Nepalese and Louisianan isolates. Accordingly, both species are formally recognized herein as novel FGSC species. *Fusarium nepalense* was resolved as the sister lineage of *Fusarium ussurianum* + *Fusarium asiaticum* within an Asian subclade of the FGSC. *Fusarium louisianense* was strongly supported as a reciprocally monophyletic sister of *Fusarium gerlachii* + *F. graminearum*, suggesting that this subclade might be endemic to North America. Multilocus Bayesian species tree analyses augment these results and provide evidence for a distinct lineage within *F. graminearum* predominately from the Gulf Coast of Louisiana. As predicted by the MLGT assay, mycotoxin analyses demonstrated that *F. nepalense* and *F. louisianense* could produce 15ADON and nivalenol, respectively, *in planta*. In addition, both species were only able to induce mild FHB symptoms on wheat in pathogenicity experiments.

Published by Elsevier Inc.

1. Introduction

Outbreaks and epidemics of Fusarium head blight (FHB) of wheat and barley, and other small grain cereals, have been reported in major production areas throughout the world since the re-emergence of this economically devastating disease in the early 1990s (Goswami and Kistler, 2004; Xu and Nicholson, 2009). FHB epidemics over the past two decades have resulted in multibillion-dollar losses to world agriculture. Two factors contribute to the economic destructiveness of this disease: (1) grain heavily contaminated with FHB mycotoxins and estrogenic metabolites such as zearalenone is unsuitable for food or feed, and (2) FHB typically results in significant reduction in grain yields and price discounting. Grain contaminated with trichothecene mycotoxins, which include deoxynivalenol (i.e., vomitoxin), nivalenol and their acetylated derivatives, pose a significant global threat to human health and food safety. In addition to being implicated in mycotoxicoses of livestock and humans (Peraica et al., 1999), trichothecene mycotoxins have been reported to alter immune function (Pestka and Smolinski, 2005) and inhibit eukaryotic protein synthesis (Ueno et al., 1973). In addition, some trichothecenes have been shown to function as virulence-associated factors on sensitive cereals (Jansen et al., 2005; Proctor et al., 1995). Multiple species within the B-trichothecene lineage of FHB pathogens (hereafter referred to as the B-clade) have been documented as causal agents of FHB, with *Fusarium graminearum* and *Fusarium asiaticum* representing the two most important species based on surveys of FHB genetic diversity throughout the world. As the name suggests, *F. asiaticum* is largely responsible for FHB in regions of China (Gale et al., 2002; Ji et al., 2007; Qu et al., 2007; Yang et al., 2008; Zhang et al., 2007), Japan (Karugia et al., 2009; Suga et al., 2008), Nepal (Carter et al., 2000, 2002; Chandler et al., 2003; Desjardins and Proctor, 2010) and Korea (Lee et al., 2009), whereas *F. graminearum*

* Corresponding author. Fax: +1 309 681 6672.
E-mail address: kerry.odonnell@ars.usda.gov (K. O'Donnell).

1087-1845/$ - see front matter Published by Elsevier Inc.
doi:10.1016/j.fgb.2011.09.002

is currently distributed panglobally (O'Donnell et al., 2000, 2004). The latter species is responsible for virtually all FHB in North America (Gale et al., 2007, 2011; Ward et al., 2008; Zeller et al., 2004), though *F. asiaticum* has been reported from the U. S. recently (Gale et al., 2011). Prior to the application of genealogical concordance phylogenetic species recognition (GCPSR, Taylor et al., 2000), *F. graminearum* was assumed to comprise a single panmictic species. However, phylogenetic analyses of DNA sequences from portions of 12 nuclear genes totaling 16 kb have revealed that this morphospecies comprises at least 14 biogeographically structured, phylogenetically distinct species, given that they satisfy the highly conservative criteria of genealogical concordance and non-discordance under GCPSR (Dettman et al., 2003; Pringle et al., 2005). For the sake of clarity, the species lineages within the *F. graminearum* species complex hereafter are collectively referred to as the FGSC. To facilitate accurate communication of FHB species diversity and pathogen identity within the scientific community, 13 of the phylogenetically distinct species within the FGSC have been described formally and given Latin binomials.

The current study was initiated to investigate species diversity and trichothecene toxin chemotype potential of three genetically novel FHB isolates from rice in Nepal and two novel isolates from wheat in Louisiana detected using different molecular markers in separate pathogen surveys (Chandler et al., 2003; Desjardins and Proctor, 2010; Gale et al., 2011.). Using a genetic screen employing randomly amplified polymorphic DNA (RAPD), sequence characterized amplified region (SCAR) marker data, and phylogenetic analyses of *Tri101* gene sequences, Chandler et al. (2003) designated three genetically novel strains collected in the mid-west district of Lamjung, Nepal in 1997 as *F. graminearum* lineage 9. Subsequently designated the Nepal lineage (Desjardins and Proctor, 2010), its genealogical exclusivity was supported by phylogenetic analyses of a 4-gene dataset. In a separate survey of FHB pathogen diversity on wheat in Louisiana conducted in 2007, Gale et al. (2011) identified two genetically novel isolates using PCR-RFLP markers. Given this background, the primary objectives of the present study were to: (1) type the five aforementioned isolates using a recently validated multilocus genotyping assay (MLGT; Ward et al., 2008) for FHB species determination and trichothecene toxin chemotype prediction, (2) assess species limits using GCPSR-based multilocus molecular phylogenetics, (3) characterize their morphological phenotypes, and (4) assess whether they could produce trichothecene toxins *in planta* and induce FHB on wheat. In addition, recently developed phylogenetic techniques have been employed to independently assess species limits. These take into account the effect that independent gene histories may have in misconstruing phylogenetic estimation via discordance among gene trees. A recent modification to the program Bayesian Evolutionary Analysis Sampling Trees (BEAST, Drummond and Rambaut, 2007), Species Tree Ancestral Reconstruction-BEAST (STAR- or ∗BEAST, Heled and Drummond, 2010) was used on the multilocus dataset to provide an estimate of the species tree with nodal support for a genetically divergent population of *F. graminearum* known predominately from the Gulf Coast of the United States (Gale et al., 2011; Starkey et al., 2007). Lastly, because the novel isolates from Nepal and Louisiana fulfill the exclusivity criterion of reciprocal monophyly under GCPSR, they are formally described herein as phylogenetically distinct species within the FGSC.

2. Material and methods

2.1. Strains, multilocus genotyping, PCR amplification and DNA sequencing

Histories of the five genetically novel FGSC isolates included in this study are provided in Table 1. After these isolates were single-spored and pure cultures were established, they were subsequently identified morphologically as members of the FGSC (Aoki and O'Donnell, 1999). To assess species identity and trichothecene chemotype potential, the isolates were run through a MLGT using a Luminex 100 flow cytometer as previously described (Ward et al., 2008). Based on the results of the MLGT assay, which indicated that the isolates might represent novel FGSC species, a 12-gene dataset (16.1 kb) was constructed and analyzed to resolve their phylogenetic relationships and species identity (Table 2). PCR amplification and DNA sequencing of the 12 loci followed published protocols (O'Donnell et al., 2000, 2004; Starkey et al., 2007; Ward et al., 2002).

2.2. Maximum parsimony (MP), maximum likelihood (ML), and Bayesian phylogenetic analyses

Raw ABI chromatograms were edited and aligned with Sequencher ver. 4.9 (Gene Codes, Ann Arbor, MI), exported as NEXUS files, and improved manually using TextPad ver. 5.1.0 for Windows (http://www.textpad.com/). To assess their evolutionary relationships, sequences from the five novel isolates were aligned with those of 67 isolates chosen to represent the known phylogenetic diversity of the B-clade (Yli-Mattila et al., 2009). Due to the presence of length variable indels within the three intergenic regions of the mating type locus (MAT), sequences from the MAT partition were aligned automatically using MAFFT ver. 6.0 (http://align.bmr.kyushu-u.ac.jp/mafft/software/). To assess whether the individual loci could be analyzed as a combined dataset, MP bootstrap values $\geqslant$70% were used as the threshold for topological concordance. Results of these conditional combinatory analyses indicated the seven individual partitions could be analyzed as a combined dataset. Unweighted MP analyses of the individual and combined datasets were conducted with PAUP ver. 4.0b10 (Swofford, 2002), employing tree-bisection and reconnection (TBR) branch swapping and 1000 random sequence additions per replicate. Nonparametric MP bootstrapping was used to assess clade support, employing 1000 pseudoreplicates of the data, 10 random addition sequences per replicate and TBR branch

Table 1
Novel FHB strains subjected to GCPSR analyses in this study.

Taxon	NRRL#	Equivalent strain numbers[a]	Host	Geographic Origin	Year Isolated
F. louisianense	54196	LRG 07-73, CBS 127524, MAFF 242710	Wheat head	Jefferson Davis Parish, Louisiana, USA	2007
F. louisianense	54197	LRG 07-100 T[b], CBS 127525, MAFF 242711	Wheat head	Jefferson Davis Parish, Louisiana, USA	2007
F. nepalense	54220	RL1 = HKM87, CBS 127669	Rice	Lamjung, Nepal	1997
F. nepalense	54221	RL2 = HKM91, CBS 127943	Rice	Lamjung, Nepal	1997
F. nepalense	54222	RL3 = HKM86 T[b], CBS 127503	Rice	Lamjung, Nepal	1997

[a] CBSs, Centraalbureau voor Schimmelcultures – Fungal Biodiversity Center, Utrecht, The Netherlands; FRC, Fusarium Research Center, The Pennsylvania State University, State College, PA; LRG, Liane R. Gale, Department of Plant Pathology, University of Minnesota, St. Paul, MN; RL/HKM, (Carter et al., 2000); MAFF, NIAS Genebank-Microorganism Section, National Institute of Agrobiological Sciences, Tsukuba, Japan.
[b] T, Ex-holotype strain.

Table 2
Tree statistics and summary of maximum parsimony phylogenetic analyses.

Locus	Number characters	Number MPTs	MPT length	CI	RI	Syn	Aut	Bootstrap support (%) *F. louisianense*	Bootstrap support (%) *F. nepalense*
α-Tubulin	1686	2	124	0.94	0.97	76	41	86	95
β-Tubulin	1337	552	120	0.79	0.87	62	30	98	99
EF-1α	648	>20,000	99	0.92	0.97	66	21	98	98
Histone H3	449	18	75	0.84	0.94	44	16	95	<70
MAT	6592	47	1064	0.84	0.94	586	251	100	100
URA-Tri101-PHO	4124	6096	735	0.80	0.91	398	160	100	100
Reductase	1273	>20,000	272	0.86	0.91	143	76	100	<70
Combined	16,109	288	2624	0.79	0.91	1378	595	100	100

Abbreviations used: MPTs, most parsimonous trees; CI, consistency index; RI, retention index; Syn, synapomorphy or parsimony informative character; Aut, autapomorphy, uniquely derived character or parsimony uninformative character.

swapping. ML analyses were implemented in GARLI ver. 0.951 (Zwickl, 2006) as previously described (O'Donnell et al., 2008), using the general-time-reversible model of nucleotide substitution with a proportion of invariant sites and gamma distributed rate heterogeneity (GTR + I + Γ). Nonparametric ML bootstrap analyses were conducted in GARLI ver. 0.951, using 1000 pseudoreplicates of the data and 5000 generations without improving the topology parameter. GCPSR-based analyses of species boundaries employed reciprocal monophyly as the exclusivity criterion (Taylor et al., 2000).

Two datasets were prepared for multilocus species tree estimation: a truncated dataset consisting of 21 isolates of *Fusarium gerlachii, Fusarium louisianense*, and canonical *F. graminearum* in concert with Gulf Coast *F. graminearum*, and a larger, 72-isolate dataset spanning the diversity of the B clade. Seven gene regions (nine intronic gene regions reduced to seven for analysis due to linkage) were subjected to a performance-based model selection analysis using DT-ModSel (Minin et al., 2003) to determine the appropriate model of nucleotide sequence evolution for each partition (Supplemental Table S1). ML phylogenetic estimation of each locus was performed using GARLI ver. 1.0 to provide preliminary visualization of individual topologies (Supplemental Fig. S3). Datasets were loaded into BEAUTi 1.6.1, which produces the XML file required for BEAST 1.6.1 (Drummond and Rambaut, 2007). Species tree ancestral reconstruction (∗BEAST) was selected, implementing the multilocus species tree estimation outlined in Heled and Drummond (2010).

Because phosphate permease (*PHO*), ammonia ligase (*URA*), and trichothecene-3-*O*-acetyltransferase (*TRI101*) are contiguous (Kimura et al., 1998; O'Donnell et al., 2000), they were analyzed as a single locus. All other partitions were assigned their own model of nucleotide sequence evolution. A Yule process was assumed as the prior for species tree generation, and a global clock was enforced across topologies. After export, the XML file was modified by hand to implement the model of nucleotide sequence evolution selected by DT-ModSel.

In order to assess the effect of priors on our analysis, trial runs were conducted under different models of nucleotide sequence evolution (GTR + I + G, HKY + I + G) in addition to runs with altered clock priors. Analyses were also run without data (i.e., sampling only from prior distributions). Subsequently, 25 individual analyses on each dataset were run for 200,000,000 generations, sampling every 10,000, on the IBEST cluster computing system at the University of Idaho. Chain convergence was assessed visually through the use of Tracer 1.5 (Rambaut and Drummond, 2007). Due to file size and resource limitations, 10 convergent runs were combined through the use of LogCombiner 1.6.1 with resampling set to 100,000 generations, and the resulting tree was annotated using TreeAnnotator 1.6.1. Trees were visualized using FigTree 1.3.1 (downloaded from tree.bio.ed.ac.uk/software/figtree/).

2.3. Phenotypic analyses, pathogenicity, and mycotoxin production in planta

Detailed analyses of morphological phenotype followed published protocols (Aoki and O'Donnell, 1999; O'Donnell et al., 2004). Holotypes of *Fusarium nepalense* (NRRL NRRL 54220 = CBS 127669) and *F. louisianense* (NRRL 54197 = CBS 127525) have been deposited as dried cultures in the US National Fungus Collection (BPI), USDA-ARS, Beltsville, MD, USA as BPI 881006 and BPI 881005, respectively. Cultures of the two novel species are available from the ARS Culture Collection (NRRL) and the Centraalbureau voor Schimmelcultures (CBS-KNAW) Fungal Diversity Center (Table 1). To assess whether the novel species could induce FHB symptoms on wheat, pathogenicity experiments were conducted, using the highly susceptible hard red spring wheat cultivar Norm (Goswami and Kistler, 2005; Starkey et al., 2007). Three replicates were conducted for each strain and ten spikes from separate plants were inoculated per replicate. Inoculum consisting of 10,000 spores in 10 μl of water and Triton-X-100 at 0.01% was introduced into the fifth, fully formed spikelet from the base of each spike. Inoculated plants were initially incubated in a humidity chamber for 48 h, after which they were transferred to a growth chamber set at 18 °C during the 16 h light period followed by 16 °C for the 8 h dark period. To assess pathogenicity, the number of spikelets showing symptomatic necrotic lesions and/or blighting was scored 2 weeks after inoculation. *F. graminearum* strain NRRL 31084 (=PH-1) was used as a positive control for scoring FHB symptoms and trichothecene toxin production *in planta*. Detailed methods for conducting toxin analyses have been published elsewhere (O'Donnell et al., 2000; Ward et al., 2002).

3. Results

3.1. Multilocus genotyping (MLGT) assay and phylogenetic analyses

When the novel isolates from Nepal ($N = 3$) and Louisiana ($N = 2$) were subjected to a MLGT assay for B-trichothecene clade species determination, positive genotypes were obtained for the B-clade and FGSC probes, however, negative signals were obtained for all of the species probes. To determine whether the isolates were nested within known species and simply harbored nucleotide polymorphisms unaccounted for in the design of the species probes or, alternatively, represented heretofore unknown species within the FGSC, multilocus DNA sequence data comprising portions of 12 genes totaling 16.1 kb/isolate (Table 2) was collected from these five isolates to assess their evolutionary relationships and species status. Maximum parsimony (MP) analyses of the seven individual partitions and the combined 12-gene dataset for 72-taxa representing the phylogenetic diversity of all known

B-clade species strongly indicated the Nepalese and Louisianan isolates represented novel FGSC species, using reciprocal monophyly as the exclusivity criterion under GCPSR (Fig. 1; Dettman et al., 2003; Taylor et al., 2000). The best ML tree received a log likelihood of −41093.14, based on 10 independent analyses of the combined dataset; the MP analysis recovered 288 equally parsimonious trees (Fig. 1), which were highly similar to the best ML tree. The novel FGSC species are formally described in Appendix A as *F. nepalense* and *F. louisianense*, based on the multilocus phylogenetic analyses and detailed phenotypic data.

3.2. F. nepalense

MP bootstrap analyses of five of the seven individual data partitions (MP-BS = ⩾86%) and the combined 12-gene dataset (MP-BS/ML-BS = 100%) provided strong support for the reciprocal monophyly of *F. nepalense* relative to the other FGSC species. Though evolutionary relationships were unresolved by analysis of the histone H3 and reductase data partitions (<70% MP-BS), they did not contradict the monophyly of this species lineage. Bootstrap analyses of the combined dataset support *F. nepalense* as a

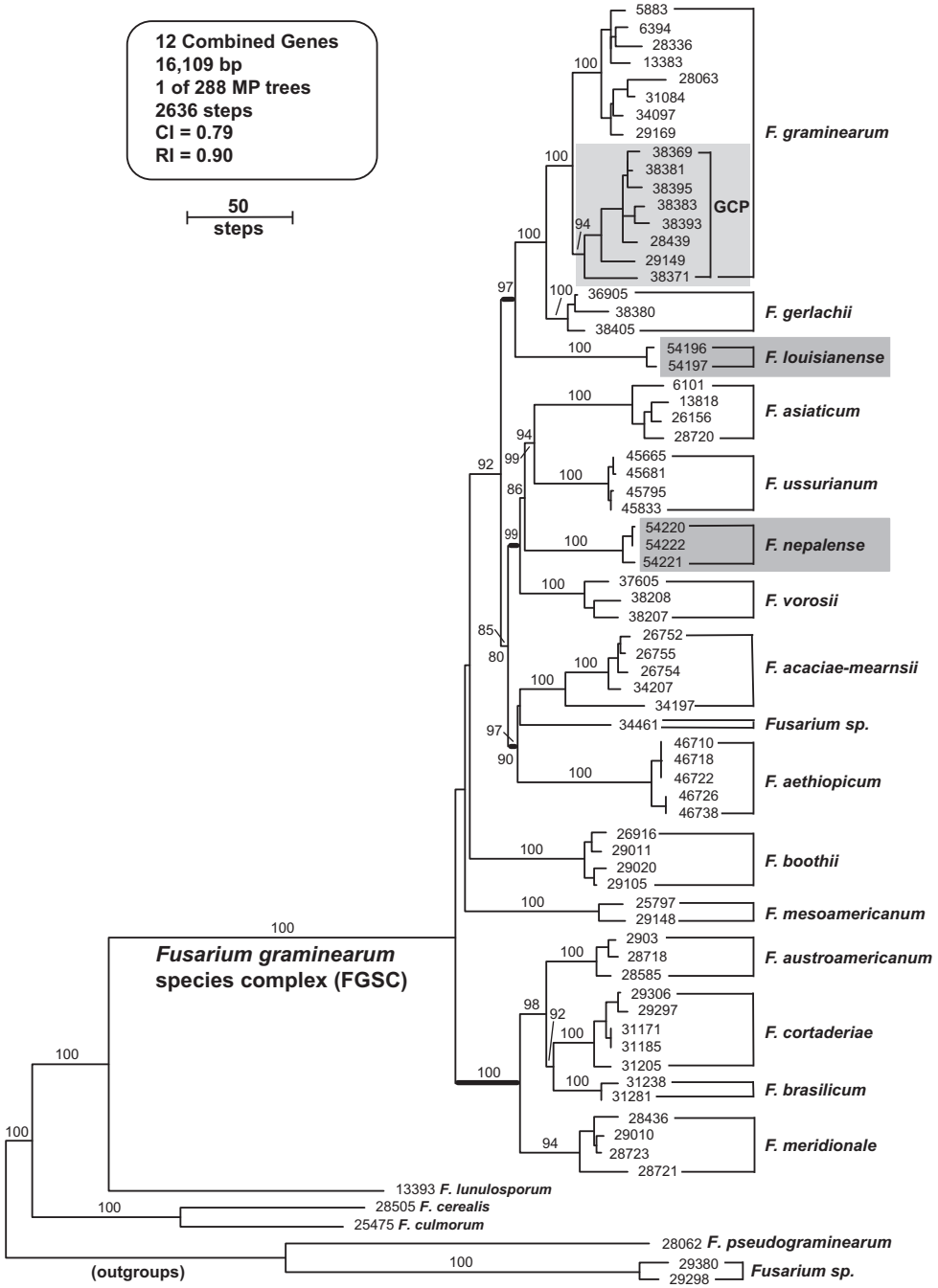

Fig. 1. Molecular phylogeny of B-type trichothecene toxin-producing fusaria inferred from portions of 12 genes comprising 16.1 kb of aligned DNA sequence data. The *F. graminearum* complex (FGSC) comprises 16 phylogenetically distinct species, including *F. nepalense* and *F. louisianense* described in this study (identified by dark grey highlight). The phylogram is one of 288 equally most-parsimonious trees inferred from the combined dataset, using sequences of *F. pseudograminearum* and *Fusarium* sp. NRRL 29298 and 29380 to root the tree. Maximum likelihood (ML) bootstrap values are indicated above nodes based on 1000 pseudoreplicates of the data. Maximum parsimony (MP) bootstrap values are only indicated if they differed by ⩾5% from the ML bootstrap value. Thick internal nodes are used to identify four strongly supported, biogeographically structured subclades within the FGSC. GCP, genetically divergent Gulf Coast population of *F. graminearum* (identified by light grey highlight).

monophyletic sister of *Fusarium ussurianum* + *F. asiaticum* (Fig. 1; ML-BS = 86%, MP-BS = 84%). In addition, strong monophyly bootstrap support was obtained (ML-BS/MP-BS = 99%) for a putatively Asian subclade consisting of (*Fusarium vorosii* (*F. nepalense* (*F. ussurianum*, *F. asiaticum*))). Collectively, these analyses indicate this species lineage has been genetically isolated from other members of the FGSC for an extended period of its evolutionary history, consistent with an advanced state of speciation. Accordingly, NRRL 54220, 54221, and 54222 are formally described as *F. nepalense* (see Appendix A), a novel species within a putatively Asian subclade of the FGSC. Morphological species recognition failed to distinguish *F. nepalense* from the Gulf Coast population of *F. graminearum* and *Fusarium* sp. NRRL 34461 (Table 3, Figs. 2A and 3). These three species produce asymmetric 5-septate macroconidia of similar length and width with a narrow apical beak and are widest above the mid-region. In pathogenicity experiments, the three strains of *F. nepalense* tested only induced mild head blight on red hard spring wheat cultivar Norm (Table 4). As predicted by the MLGT assay, they produced 15-acetyldeoxynivalenol as the primary acetyl-ester of deoxynivalenol *in planta* (15ADON chemotype; Table 4).

3.3. F. louisianense

The two isolates of this species (NRRL 54196 = LRG 07-73, NRRL 54197 = LRG 07-100; Table 1) were discovered initially using novel PCR-RFLP markers during a survey of head blight of wheat conducted in Jefferson Davis Parish, Louisiana in 2007 (Gale et al., 2011). To date, no other isolates of this species have been discovered. The genealogical exclusivity of these two isolates was strongly supported by all seven individual data partitions (MP-BS = ⩾85%) and the combined dataset (MP-BS/ML-BS = 100%). In addition, *F. louisianense* was strongly supported (MP-BS = 98%, ML-BS 97%) as a monophyletic sister group to *F. gerlachii* + *F. graminearum* in the combined 12-gene phylogeny (Fig. 1). The genetic isolation of *F. louisianense* from the other FGSC species, reflected by the strong monophyly bootstrap support for its genealogical exclusivity (Table 2), show this evolutionary lineage fulfills the highly conservative criteria of genealogical concordance and nondiscordance under GCPSR (Dettman et al., 2003). Therefore, NRRL 54196 and 54197 are formally described herein as *F. louisianense*. This species can be distinguished from other B-clade species by its morphologically unique 5-septate macroconidia (Table 3, Figs. 2B and 3). The two isolates of *F. louisianense* tested only induced mild FHB symptoms on wheat in a greenhouse experiment, using the highly susceptible hard red spring cultivar Norm as the host (Table 4). In addition, consistent with the trichothecene chemotype predicted by the MLGT assay, mycotoxin analyses demonstrated that both strains produced nivalenol *in planta* (NIV chemotype; Table 4).

Table 3
Pathogenicity and toxin accumulation in wheat infected with strains of *F. louisianense* or *F. nepalense*.

Strain[c]	Trichothecene concentration (ppm)[a]			Pathogenicity[b]
	DON	15ADON	Nivalenol	
PH-1 (*Fg*)	352.7 ± 94.9	47.3 ± 16.6	nd	9.2 ± 0.1
NRRL 54196 (*Fl*)	nd	nd	4.6 ± 5.0[a]	1.1 ± 0.2[d]
NRRL 54197 (*Fl*)	nd	nd	4.7 ± 6.3[a]	1.0 ± 0.0[d]
PH-1 (*Fg*)	476.3 ± 79.8	41.7 ± 11.2	nd	9.0 ± 1.1
NRRL 54220 (*Fn*)	160.3 ± 86.9	10.6 ± 6.8	nd	2.7 ± 1.8[d]
NRRL 54221 (*Fn*)	264.1 ± 131.8	29.3 ± 19.3	nd	4.1 ± 2.0[d]
NRRL 54222 (*Fn*)	167.2 ± 196.7	10 ± 12.4	nd	1.4 ± 0.6[d]

[a] Means and standard deviation of trichothecene concentration in wheat spikelets (cultivar Norm), 14 days after inoculation. nd, none detected.
[b] Mean and standard deviation of symptomatic spikelets arising from a point inoculation after 14 days on wheat cultivar Norm.
[c] All results compared with PH-1, the sequenced reference strain of *F. graminearum* (*Fg*). (*Fl*), *F. louisianense*; (*Fn*), *F. nepalense*.
[d] Means were compared using 2-tailed Student's *t*-tests with unequal variance, P = 0.01. Letters indicate means that are significantly different.

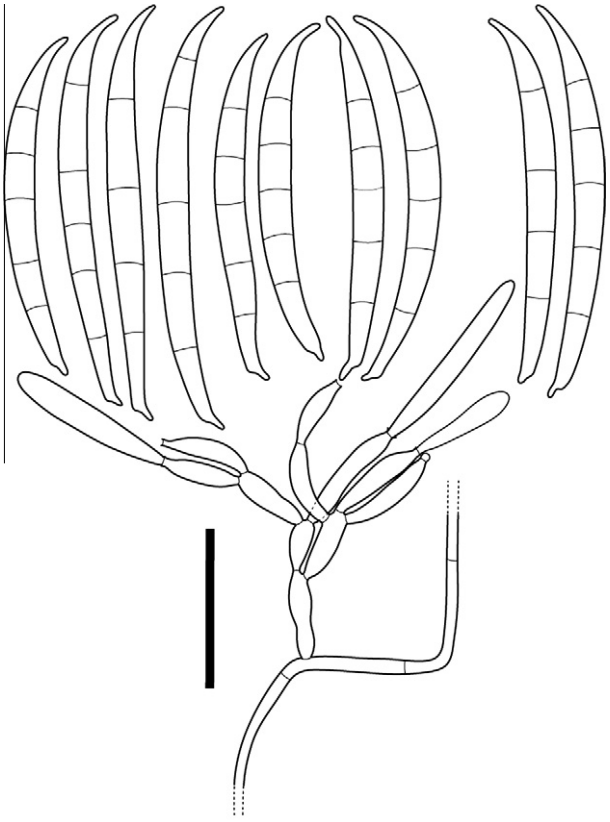

Fig. 2A. *Fusarium nepalense* (NRRL 54221). Phialidic conidiophore and 4–5 septate sporodochial conidia formed from monophialides on a branched conidiophore on SNA under black light. Conidia are gradually curved, typically widest above the mid-region and possess a prominent foot cell and a narrow apical beak.

3.4. Design of F. nepalense and F. louisianense species probes for the MLGT assay

Based on the results of the present study, the MLGT assay for B-clade species determination and trichothecene toxin chemotype prediction (Ward et al., 2008) was updated by adding two species probes for *F. louisianense* and one for *F. nepalense*. The *F. louisianense* probes (EFLa(41)-TTACTACACAATATACTCATCAATGCCCTCTCCCCACAAACCAC and ATLa(48)-AAACAAACTTCACATCTCAATAATAACTTCATCAAGGGCGGACTT) target species-specific nucleotide polymorphism within *EF-1α* and *Tri101*, respectively, whereas the *F. nepalense* species probe (EFnep(8)-ATTCCTTTTACATTCATTACTTACCACGACGACTCGATACGT) was designed based on variation identified within *EF-1α*. A unique sequence tag (underlined) was appended to the 5′ end of each species probe so that the allele-specific extension products could be sorted by hybridization with fluorescent microspheres (Luminex Corporation) as previously described (Ward et al., 2008). To validate the updated MLGT assay, isolates of *F. louisianense* and *F. nepalense* were run together with an isolate panel comprising the 66 B-clade isolates used in the design and validation of previously published versions of the MLGT assay (O'Donnell

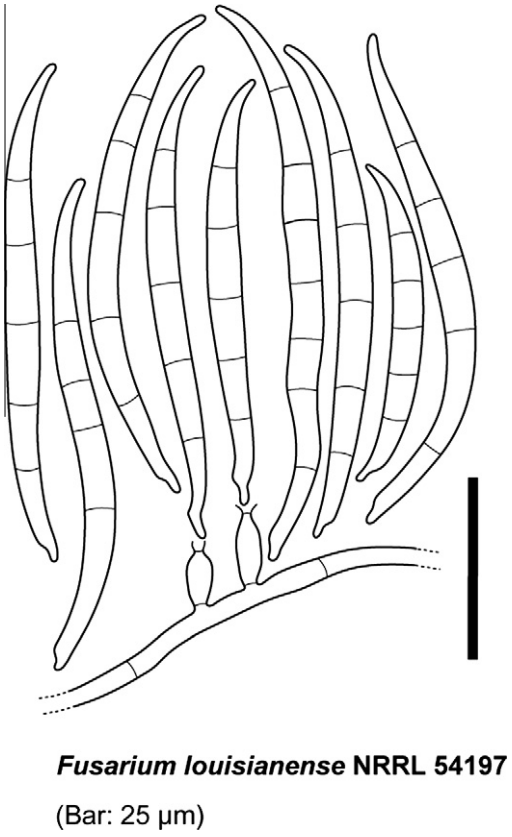

Fig. 2B. *Fusarium louisianense* (NRRL 54197). Monophialidic conidiophore and 4–5 septate sporodochial conidia formed on SNA under black light. Conidia are gradually curved, typically widest at the mid-region and possess a prominent foot cell but lack a narrow apical beak.

et al., 2008; Ward et al., 2008; Yli-Mattila et al., 2009). Fluorescence intensity values obtained using the *F. louisianense* and *F. nepalense* probes were at least 25 times higher than the highest values recorded for the other B-clade species.

3.5. Species status of the F. graminearum Gulf Coast population (GCP) and Bayesian inference of the B clade

Initial analyses that altered prior distributions did not have any effect on the relationships observed in preliminary species trees. Runs that sampled only from the prior (i.e., without data) revealed that the priors themselves were not influencing the posteriors, an essential test to make sure that the data and not the priors themselves were governing the results. Choosing the incorrect model of nucleotide sequence evolution produced a low effective sample size (ESS) for parameters that do not exist in the data but did not influence qualitative relationships among species, the sole parameter of interest in this study. The combined analyses resolved Gulf Coast isolates of *F. graminearum* as sister to the canonical *F. graminearum* with >0.99 posterior nodal support in both analyses. The relationship (((Gulf Coast population, *F. graminearium*) *F. gerlachii*) *F. louisianense*) was also reinforced in both analyses with high nodal support (Fig. 4). ML gene trees show varying levels of resolution among loci. Resolution ranges from MAT, which has significant structure, to reductase, which has poor resolution and little structure. Nevertheless, several show structure differentiating the GCP *graminearum* from the canonical *F. graminearum* lineage (Supplemental Fig. S1). Relationships among other species in the B clade have mixed nodal support, though some are well resolved. Some relationships are in conflict with the concatenated ML and MP trees, but the nodes supporting these resolutions have low posterior support; this is a result of the uninformativeness of some loci used in this analysis (Fig. 5).

4. Discussion

4.1. Phylogenetic analysis

The primary objective of the present study was to assess phylogenetic relationships, species status and trichothecene toxin chemotype diversity of three genetically novel FHB strains recovered from blighted rice in Nepal in 1997 and two strains isolated from symptomatic wheat in Louisiana. Because these isolates were

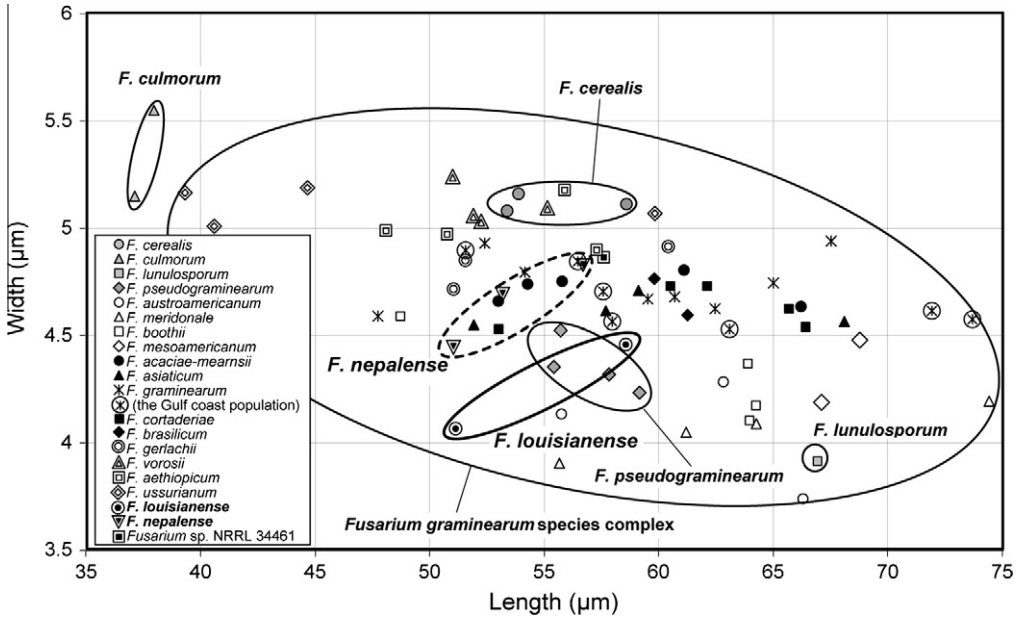

Fig. 3. Length and width of 5-septate conidia of B-clade species produced under black light. Isolates of *F. nepalense* and *F. louisianense* are indicated, respectively, by a triangle and circle with a solid dot. The oval circumscribing the two isolates of *F. louisianense* and three isolates of *F. nepalense* graphically illustrate conidial length and width cannot be used to identify these species.

Table 4
Conidial morphology characteristic of B trichothecene toxin-producing clade fusaria[a].

Species	Width of 5-septate conidia (average value in μm)	Longitudinal axis of conidia	Narrow apical beak (±)	Upper and lower half of conidia	Widest region of conidia
F. lunulosporum	<4.5	Curved	+	Symmetric	Mid-region
F. austroamericanum	<4.5	Typically straight	±	Asymmetric	Mid-region
F. boothii	<4.5	Gradually curved	+	Mostly symmetric	Mid-region
F. meridonale	<4.5	Gradually curved	+	Mostly symmetric	Mid-region
F. mesoamericanum	4–4.5	Typically straight	–	Asymmetric	Above mid-region
F. louisianense	4–4.5	Gradually curved	–	Asymmetric	Mid-region
F. pseudograminearum	4–4.5	Curved	+	Symmetric	Mid-region
F. acaciae-mearnsii	4.5–5	Gradually curved	+	Asymmetric	Below mid-region[b]
F. brasilicum	4.5–5	Straight or gradually curved	+	Asymmetric	Below mid-region
F. cortaderiae	4.5–5	Straight or gradually curved	+	Asymmetric	Below mid-region
F. gerlachii	4.5–5	Gradually curved	+	Asymmetric	Mid-region
Fusarium sp. NRRL34461	4.5–5	Gradually curved	+	Asymmetric	Above mid-region[b]
F. nepalense	4.5–5	Gradually curved	+	Asymmetric	Above mid-region
F. graminearum (Gulf Coast)	4.5–5	Gradually curved	+[c]	Asymmetric	Above mid-region
F. graminearum	4.5–5	Gradually curved	–[c]	Asymmetric	Above mid-region
F. asiaticum	4.5–5	Gradually curved	–	Asymmetric	Above mid-region
F. aetiopicum	≃5	Gradually curved	–	Asymmetric	Above mid-region
F. vorosii	>5	Straight or gradually curved	±	Asymmetric	Above mid-region
F. ussurianum	>5	Curved	+	Symmetric	Above mid-region
F. cerealis	>5	Curved	+	Symmetric	Mid-region
F. culmorum	>5	Curved	–	Symmetric	Mid-region

[a] When using the combined conidial characters, the following six species and four species groups could be distinguished within the FGSC: *F. austroamericanum*, *F. mesoamericanum*, *F. louisianense*, *F. acaciae-mearnsii*, *F. gerlachii*, *F. ussurianum*, *F. boothi* + *F. meridionale*, *F. brasilicum* + *F. cortaderiae*, *Fusarium* sp. NRRL 34461 + *F. nepalense* + *F. graminearum* (Gulf Coast), *F. graminearum* + *F. asiaticum* + *F. aetiopicum* + *F. vorosii*.

[b] A single strain of *Fusarium* sp. NRRL 34461, forming asymmetric conidia widest above mid-region, was previously considered as a unique strain of *F. acaciae-mearnsii* (Starkey et al., 2007).

[c] Strains of the divergent Gulf Coast population of *F. graminearum* were unique in that they produced conidia with a narrow apical beak.

previously characterized as genetically divergent, using different sets of molecular markers (Carter et al., 2000, 2002; Chandler et al., 2003; Desjardins and Proctor, 2010; Gale et al., 2011), we conducted GCPSR-based multilocus phylogenetic analyses to rigorously assess their species identity (Dettman et al., 2003; Taylor et al., 2000). One of the most important findings to emerge from these analyses is the Nepalese and Louisianan isolates both fulfill the requirements of phylogenetic species recognition, employing the highly conservative operational criteria of genealogical concordance and non-discordance under GCPSR (Pringle et al., 2005). Specifically, both species were resolved as reciprocally monophyletic in bootstrap analyses of the majority of the individual data partitions and the combined 12-gene dataset, and their genealogical exclusivity was not contradicted by bootstrap analyses of any locus. The genealogical concordance and non-discordance observed indicates they have been genetically isolated from other members of the FGSC over an extended period of evolutionary time, thereby supporting the formal recognition of *F. nepalense* and *F. louisianense* as novel head blight species (see Appendix A).

4.2. F. nepalense

Results of the present GCPSR-based study strongly support the findings of Chandler et al. (2003) and Desjardins and Proctor (2010), who used diverse molecular markers to identify strains from blighted rice collected in Lamjung, Nepal in 1997 as a distinct lineage. Following the designation used at the time for the eight known phylogenetic species within the FGSC (O'Donnell et al., 2000; Ward et al., 2002), Chandler et al. (2003) described these strains as lineage 9 of *F. graminearum*. Subsequently, these strains were designated the Nepal lineage based on phylogenetic analyses of a four-gene dataset (Desjardins and Proctor, 2010). Here we extend these studies by showing that this lineage is strongly supported as reciprocally monophyletic with respect to the other FGSC species. The failure of morphological species recognition to distinguish *F. nepalense* from two other FGSC species (Table 3) is concordant with those on other agriculturally and medically important fungi (reviewed in Taylor et al., 2000, 2006) which suggest that cryptic speciation often goes undetected due to the inherent limitations of morphological species recognition.

Given the advanced state of speciation indicated by the genealogical concordance and non-discordance of this species lineage, we formally recognize *F. nepalense* as a novel phylogenetically distinct species within a putatively Asian subclade of the FGSC. The biogeographic structure exhibited by the four species within this subclade suggests that they may have evolved allopatrically within Asia. While *F. asiaticum* has been reported to be more prevalent in southern regions of China and Japan (Gale et al., 2002; Qu et al., 2007; Suga et al., 2008; Yang et al., 2008; Zhang et al., 2010), *F. ussurianum* is currently only known for the Far East of Russia, and *F. vorosii* appears to be largely restricted to the Far East of Russia and Hokkaido, Japan (Starkey et al., 2007; Yli-Mattila et al., 2009), although the first isolate of the latter species was initially discovered in Hungary (Tóth et al., 2005). Assessing whether *F. nepalense* is endemic to Nepal will require additional sampling to identify its phylogeographic distribution. Thus far, *F. nepalense* has only been found in the central Nepalese districts of Lamjung ($N = 35$) and Kaski ($N = 1$), and the western district of Dailekh ($N = 2$) where it was isolated from crop debris ($N = 12$), rice ($N = 11$), maize ($N = 8$), weeds ($N = 5$) and wheat ($N = 2$) (Desjardins and Proctor, 2010). However, because published surveys of head blight in Nepal have identified at least two non-indigenous FGSC species (i.e., *F. boothii* and *Fusarium meridionale*; Chandler et al., 2003; Desjardins and Proctor, 2010; O'Donnell et al., 2000, 2004), it is possible that subsequent studies may reveal that *F. nepalense* was introduced to Nepal from some other region of Asia.

F. asiaticum and *F. meridionale* appear to represent the two most important FGSC pathogens in Nepal, followed by *F. nepalense* which comprised 39 of the 252 isolates genotyped by Desjardins and Proctor (2010). Although the three isolates of *F. nepalense* from rice were only able to induce mild head blight symptoms on the highly susceptible hard red spring wheat cultivar Norm, testing of additional isolates may identify ones that are highly virulent, given that previous studies have shown pathogenicity to wheat can vary

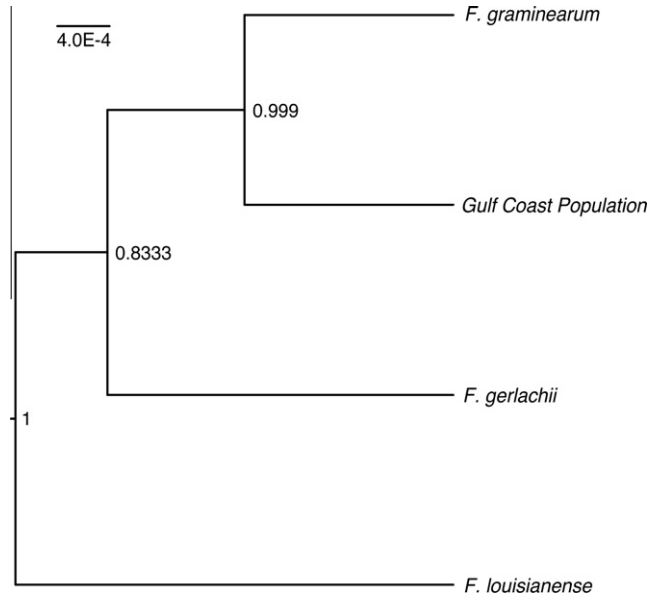

Fig. 4. Maximum clade credibility tree from the 21-taxa dataset. Tree was annotated using a posterior probability limit of 0.5 in TreeAnnotator. Posterior nodal support values are listed next to their respective nodes. Note that the Gulf Coast population and *F. graminearum* form a clade with high posterior support.

greatly within the FGSC species (Goswami and Kistler, 2005; O'Donnell et al., 2000, 2004).

4.3. F. louisianense

Our working biogeographic hypothesis, based on the strong monophyly bootstrap support for a (*F. louisianense* (*F. gerlachii*, *F. graminearum*)) subclade (ML-BS = 97%), is that these three species may have evolved allopatrically within North America. We base this speculation on the fact that the former species is currently only known from Louisiana, the Gulf Coast population of *F. graminearum* has only been recovered from Florida, Louisiana, Ohio and Indiana (Gale et al., 2011; O'Donnell et al., 2000), and *F. gerlachii* appears to be restricted to the upper Midwest of the US (Starkey et al., 2007). Additional head blight pathogen surveys that include collections from non-graminaceous hosts are needed to test this hypothesis and increase our understanding of their host range, geographic distribution and mycotoxin potential. In contrast to *F. graminearum*, which is the most important FHB pathogen within North America, and most other regions of the world (O'Donnell et al., 2000, 2004, 2008; Starkey et al., 2007; Ward et al., 2002; Yli-Mattila et al., 2009), neither *F. louisianense* nor *F. gerlachii* currently appear to pose a significant threat to cereal production within the US. However, because both species have been shown to elaborate nivalenol *in planta*, which has been reported to be considerably more toxic to humans and other animals than deoxynivalenol (Minervini et al., 2004), proactive molecular surveillance of both pathogens seems prudent to alert disease control specialists of any significant increase in their population sizes.

Although the two isolates of *F. louisianense* only induced mild head blight symptoms on wheat in growth chamber tests, it is reasonable to assume that more virulent isolates of this species may be found, given the wide variation in aggressiveness reported for several of the FGSC species (Goswami and Kistler, 2005). Additional isolates of *F. louisianense* are also needed to document the full range of its pathogenic and phenotypic variation, host range and geographic distribution. However, the available data indicates the morphologically unique 5-septate macroconidia produced by *F. louisianense* can be used to distinguish it from the other B-clade species (Table 3).

4.4. Species status of the F. graminearum Gulf Coast population (GCP) and Bayesian inference of B clade

Historically, large numbers of gene regions have been concatenated into large data matrices prior to phylogenetic analysis. However, concatenation removes the impact of discordant histories among gene regions by assuming a single model of sequence evolution and a uniform set of evolutionary influences. Recently, several approaches have been implemented that take partitioned data into account for species tree estimation. ML methods that use vectors of gene trees as input (i.e., STEM, Kubatko et al., 2009) and Bayesian implementations that co-estimate distributions of species trees and gene trees (i.e., BEST, Edwards et al., 2007, and ∗BEAST, Heled and Drummond, 2010) are being used more frequently to study complex datasets (i.e., Knowles and Kubatko, 2010).

This study used ∗BEAST to provide an independent measure of support for relationships among the FGSC. A high posterior probability was observed for the node separating the GCP from *F. graminearum* in both analyses. Our working hypothesis is that the shared polymorphisms previously observed in three of the eight allelic genealogies likely reflect a speciation event that has occurred too recently to allow complete sorting of shared polymorphism due to drift (Starkey et al., 2007). However, population-level studies are needed to assess whether the genealogical discord is due to contemporary gene flow. Multilocus species tree estimation is shown to be fruitful for species-level resolution when some gene trees do not have enough information to satisfy criteria of the GCPSR by themselves (i.e., concordance cannot be assessed due to the presence of polytomies, Supplemental Fig. S1). Other methods of combining data (i.e., concatenation) may also be employed (see below). It is worth noting that ∗BEAST requires that individuals be assigned into species *a priori*. Based on morphological, ML, and MP analyses, we feel justified in our classifications of individuals to species groups. Assignment of individuals into species *a posteriori* is an active field of research (e.g., O'Meara, 2009) and may benefit this system in the future. For now, the GCPSR approach continues to be fruitful for species delineation in this group.

The 72-taxon dataset provides initial insight into multilocus Bayesian inference within the B clade. Many nodes in the species tree have low posterior nodal support, in contrast with the MP and ML analyses in which relationships were nearly fully resolved and species monophyly was strongly supported by bootstrapping. This is not entirely unexpected given that gene trees constructed in both Bayesian and Maximum Likelihood frameworks vary in the amount of resolution they provide. Larger partitions, such as the combined *PHO-Tri101-URA* region and the mating type locus, provide better resolution than the smaller partitions, which are mostly unresolved (data not shown). As a result, nodal support is lower because there is less reinforcement of many bifurcations among topologies. This has been described previously for situations where phylogenetic signal may be hidden in partitioned analysis but revealed through concatenated analysis (Sullivan, 1996). Therefore, the ML and MP tree inferred from the combined 12 gene dataset (Fig. 1) is taken as our working hypothesis of phylogenetic relationships within the FGSC because: (1) it contained much higher measures of bootstrap support than the individual partitions, and (2) the genealogical concordance observed indicates the topology accurately reflects the underlying phylogeny.

Hillis and Dixon (1991) have noted that resolving different levels of relationships in phylogenies requires genes that have different levels of divergence and, hence, different rates of evolution. It may prove fruitful to expand the B clade dataset to include genes that are known to be slowly and quickly evolving in order to resolve deep

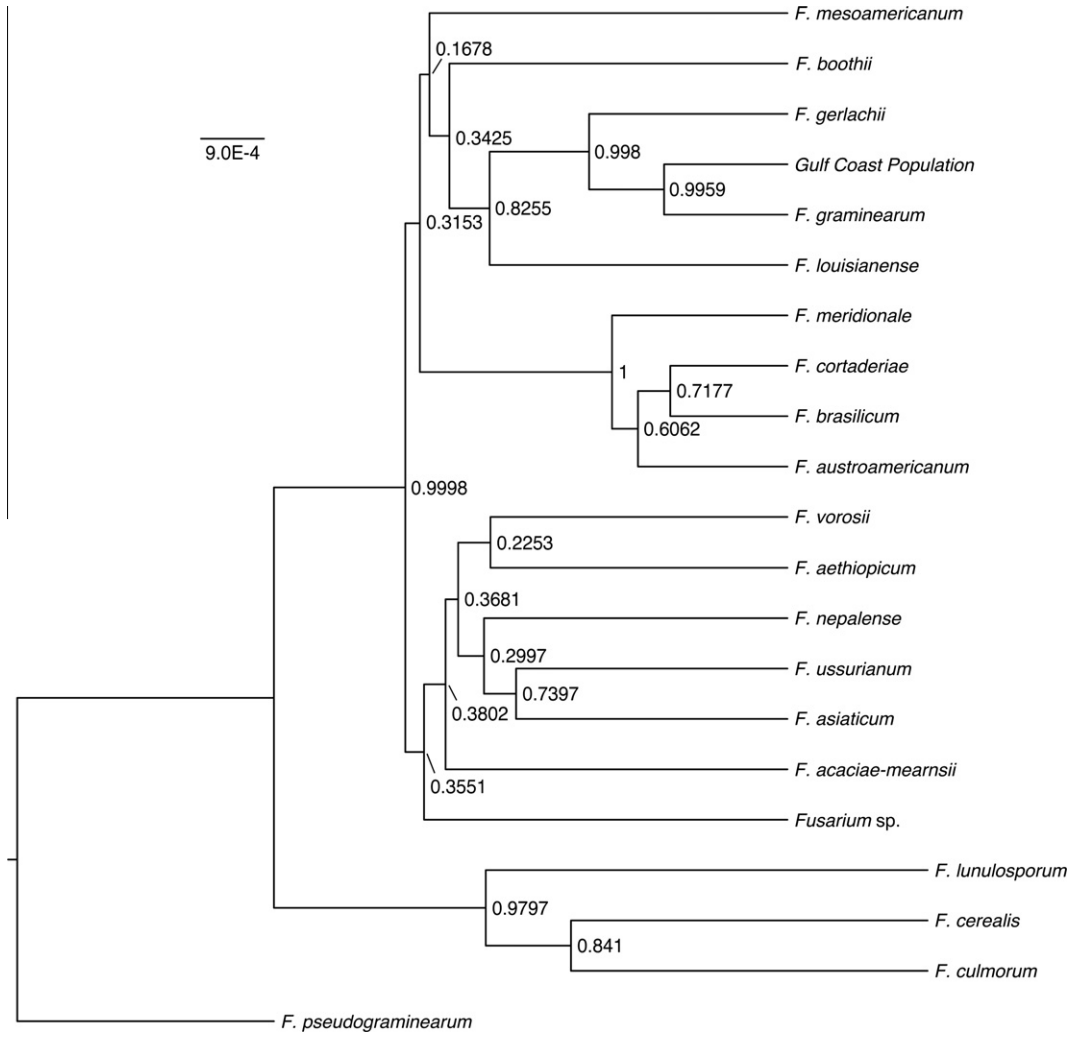

Fig. 5. Maximum clade credibility tree from the 72-taxa dataset. TreeAnnotator was used to annotate the tree using a posterior probability limit of 0.5. Values listed next to nodes represent posterior nodal support. Nodal support differs across the tree, with some well-established relationships having high posterior probabilities (i.e., the Gulf Coast population + *F. graminearum*).

and tip nodes, respectively. When gene regions have different evolutionary histories, inclusion of additional gene regions can be used to obtain a more reliable estimate of a multilocus species tree. Discovery of these regions will be expedited by the fact that entire genomes for several fusaria within the B clade either have been or currently are being sequenced (Cuomo et al., 2007; http://www.fgsc.net/Fusarium/Fusarium_workshop_2011.htm). In addition, new techniques that assume discordance among gene trees is due to hybridization (i.e., Meng and Kubatko, 2010) may prove enlightening; two examples of interspecific hybridization within the FGSC have been documented to date (Boutigny et al., 2011; O'Donnell et al., 2000).

4.5. Concluding remarks

The present GCPSR-based study has helped refine hypotheses of sister group relationships, species diversity, and the historical biogeography of the FGSC. The genealogical exclusivity of *F. nepalense* and *F. louisianense* indicates that they have been evolving as independent evolutionary lineages in the absence of significant interspecific gene flow over an extended period of evolutionary time. The available data clearly shows that biological species recognition (BSR) is a poor predictor of species limits within the FGSC. Contrary to BSR's prediction that hybridization might be common in nature, the results of multiple FHB field surveys indicate that interspecific hybrids appear to be exceedingly rare, even where multiple FGSC species are sympatric (Boutigny et al., 2011; Desjardins and Proctor, 2010; Gale et al., 2011; Lee et al., 2009; Suga et al., 2008). Similarly, morphological species recognition has limited utility within the FGSC due to the near absence of morphological apomorphies. Fortunately, genealogical concordance and non-discordance under GCPSR have proven to provide robust criteria for identifying the limits of 'biological' species within diverse fungi (reviewed in Taylor et al., 2000, 2006), including the extensive cryptic speciation detected within the B-clade.

The whole-genome sequence of several fusaria, including *F. graminearum* (Cuomo et al., 2007), should be extraordinarily useful in identifying a diverse set of phylogenetically informative orthologous genes for improving resolution within the FGSC (Marthey et al., 2008) and SNPs for population-genetic studies and molecular diagnostics. Looking to the future, when the whole genome sequence of other members of the B-clade become available, comparative genomic analyses may provide invaluable insights into the evolutionary forces that contribute to and accompany cladogenesis, as well as ultimately help identify genes that help drive the speciation process (Anderson et al., 2010; Dettman et al., 2010).

As our understanding of cryptic speciation within the FGSC increases, so too does the challenge it poses to quarantine officials

and plant disease specialists charged with preventing the inadvertent introduction of foreign FHB pathogens into non-indigenous areas. The multilocus DNA sequence data analyzed in the present study have been uploaded to FUSARIUM-ID (http://isolate.fusariumdb.org) and the Centraalbureau voor Schimmelcultures (CBS-KNAW) Fungal Biodiversity Center's website *Fusarium MLST* (http://www.cbs.knaw.nl/fusarium) to facilitate identifications of fusaria via the Internet (Geiser et al., 2004; O'Donnell et al., 2010; Park et al., 2010). Currently, the updated allele-specific MLGT assay provides the only means by which the 21 B-clade species, and their trichothecene chemotypes, can be identified accurately using a high-throughput molecular diagnostic platform. However, as knowledge gained from global FHB surveys improves our ability to more accurately predict FGSC species distributions on increasingly finer geographic scales, it should be possible to develop novel PCR-based molecular diagnostic assays that target only the species predicted to inhabit the area of interest. Given the real potential for world trade of cereals and other agricultural commodities to inadvertently introduce more vigorous and toxigenic pathogen populations into non-indigenous areas (Ward et al., 2008), coordination of programs for the global molecular surveillance of FHB pathogens are critical to minimize and reduce the threat of this economically devastating disease to the world's food supply.

Acknowledgments

Special thanks are due Stacy Sink and Nathane Orwig for excellent technical support and Yanhong Dong, Mycotoxin Laboratory, University of Minnesota, for the GC/MS mycotoxin analyses. BAJS specifically thanks Joseph Brown, Jack Sullivan, David Tank, Luke Harmon, and Travis Hagey for helpful discussion. IBEST Bioinformatics facilities are supported by NIH/NCRR P20RR16448 and P20RR016454. LRG and HCK acknowledge that a portion of this research was supported by the US Department of Agriculture under Agreement No. 59-0790-7-074, a cooperative project of the US Wheat & Barley Scab Initiative. The mention of firm names or trade products does not imply that they are endorsed or recommended by the US Department of Agriculture over other firms or similar products not mentioned. The USDA is an equal opportunity provider and employer.

Appendix A. Species descriptions

F. nepalense T. Aoki, Carter, Nicholson, Kistler & O'Donnell, sp. nov.

MycoBank MB519883 Figs. 2A and 3

Coloniae in PDA in obscuritate ad 20 °C 1.0–4.7 mm et ad 25 °C 1.6–5.8 mm in dies crescent, albae, rosea, griseo-rubrae, rubro-albae, aurantino-albae; pigmentum reversum albae, rubrae, saturato-rubrae, rubro-brunneum, brunneo-rubrae, brunneo-violaceae, violaceo-brunneae; nonnunquam cum exudatis luteolis in pagina coloniae. Odor absens vel mucidus, nonnunquam dulcis. Mycelium aerium in PDA generaliter copiosum, nonnunquam sparse formans, laxe vel dense floccosum, album, rubro-album, pallido-rubrum vel griseo-rubrum, griseo-aurantinum. Chlamydosporae et sclerotia absentes. Sporulatio in SNA sub illuminationem nigram praecox et copiosa, in conidiophora ex hyphis oriunda vel in sporodochiis in superficie agari aggregata; in obscuritate tarda et parka sporodochia copiose vel sparse formantia. Conidiophora ramose vel simplicia, in monophialides exeuntia; vel pro monophialidibus ex hyphis oriundis omissa Phialides simplices, subulatae, ampulliformes vel subcylindricae, monophialidicae. Conidia monomorphica, typice falcata et curvata, dorsiventralia, frequentissime latissima in medio aliquanto superiore, utrinque angustatae et gradatim curvata, com cellulis apicalibus arcuatis rostratis et cellulis basilaribus pediformibus, cum dimidiis superis et inferis asymmetricis, (3-)4–5(-7)-septata; conidia 5-septata sub illuminationem nigram 35.5–71 × 3.5–5 μm. Positio systematica per DNA sequentiis [α-tubulini, β-tubulini, *EF-1α*, HIS, MAT, reductasi, *URA*, *Tri101* et *PHO*] a speciebus similibus differens.

Colonies in darkness on PDA showing slow average growth rates per day of 1.0–4.7 mm at 20 °C and 1.6–5.8 mm at 25 °C. Colony color on PDA white, pink, grayish-red, reddish-white, orange-white; reverse pigmentation white, red, deep-red, reddish-brown, brownish-red, brownish-violet, violet-brown; sometimes with yellowish exudates on the surface of the colony. Colony margin entire to undulate, often forming colony sectors of different growth rates. Odor absent or moldy, some sweetish. Aerial mycelium on PDA generally abundant, sometimes sparsely developed, loosely to dense floccose, white, reddish-white, pale red to grayish red, grayish-orange. Hyphae on SNA 1.5–6.5 μm wide. Chlamydospores and sclerotia absent. Sporulation on SNA under black light quick and abundant, starting within a few days from conidiophores formed directly on hyphae or aggregated in sporodochia on the agar surface, in darkness retarded and few; sporodochia formed abundantly or sparsely. Conidiophores branched or unbranched, terminating with monophialides on the apices, or abbreviated as single monophialides formed on substrate hyphae. Phialides simple, subulate, ampulliform to subcylindric, monophialidic. Conidia of a single type, typically falcate and curved, dorsiventral, most frequently widest slightly above the midregion of their length, tapering and gradually curving toward both ends, with an arcuate and beaked apical cell and a distinct basal foot cell, upper and lower halves asymmetric, (3-)4–5(-7)-septate. Under black light, 5-septate conidia: 35.5–71 × 3.5–5.5 μm in total range, 51.0–56.7 × 4.5–4.8 μm on average, (ex-type strain: 35.5–53.2–71 × 4–4.7–5.5 μm). Based on analyses of the seven individual partitions (α-tubulin, β-tubulin, *EF-1α*, HIS, MAT, reductase, *URA*, *Tri101* and *PHO*) and combined dataset, *F. nepalense* was reolved as phylogenetically distinct from other FGSC species.

HOLOTYPUS: BPI 881006, a dried culture, isolated from rice seed, *Oryza sativa* L., Lamjung, Nepal in 1997, deposited in the herbarium of BPI (US National Fungus Collection, Beltsville, MD), USA. Ex holotype culture: NRRL 54222 = CBS 127503. Other strains examined: NRRL 54220 = CBS 127669, Nepal in 1997; NRRL 54221 = CBS 127943, Nepal in 1997.

Etymology: The epithet *nepalense* refers to the type locality country, Nepal.

Distribution: currently only known from Nepal.

Five-septate conidia formed by *F. nepalense* on SNA (Figs. 2A and 3) were indistinguishable from *Fusarium* sp. NRRL 34461, a putative new species from soil collected in Umyaka, South Africa (O'Donnell et al., 2008), and the Gulf Coast population of *F. graminearum*. These three species produced conidia under black light that were wider than 4.5 μm on average, the widest region was above the midregion and they possessed a narrow apical beak (Table 3). Two strains of *F. nepalense*, NRRL 54221 and NRRL 54222, grew faster on PDA, i.e., 3.8–4.7 mm/day at 20 °C and 3.9–5.8 mm/day at 25 °C on average, and formed abundant aerial mycelia, as observed in most species within the *FGSC*. Strain NRRL 54220, however, grew slowly on PDA, i.e., 1.0 mm/day at 20 °C and 1.6 mm/day at 25 °C on average and formed less abundant aerial mycelia. Delimitation of *F. nepalense* was strongly supported using the exclusivity criterion under GCPSR. *F. nepalense* formed a strongly supported putatively Asian clade which included *F. asiaticum*, *F. ussurianum* and *F. vorosii* in the multilocus phylogeny (Fig. 1).

Fusarium louisianense Gale, Kistler, O'Donnell & T. Aoki, sp. nov.

MycoBank MB519884 FIGS. 2B and 3

Coloniae in PDA in obscuritate ad 20 °C 0.8–0.9 mm et ad 25 °C 1.3–1.7 mm in dies crescent, roseo-albae vel rubro-griseae, pallido-rubrae vel griseo-rubrae; pigmentum reversum rubro-brunneum vel obscuro-brunneum. Odor absens vel mucidus. Mycelium aerium in PDA vix copiosum, dense floccosum vel pannosum, album vel rubro-album, pallido-rubrum vel griseo-rubrum. Chlamydosporae et sclerotia absentes. Sporulatio in SNA in obscuritate et sub illuminationem nigram copiosa, in conidiophora ex hyphis oriunda vel in sporodochiis in superficie agari aggregata; sporodochia copiose formantia. Conidiophora ramosa, verticillata vel simplicia, in monophialides exeuntia; vel pro monophialidibus ex hyphis oriundis omissa. Phialides simplices, subulatae, ampulliformes vel subcylindricae, monophialidicae. Conidia monomorphica, typice falcata et gradatin curvata, nonnunquam sigmoidea vel aliquanto recta, dorsiventralia, frequentissime latissima in medio, utrinque angustatae et curvata, com cellulis apicalibus arcuatis et cellulis basilaribus pediformibus, cum dimidiis superis et inferis asymmetricis, (3-)4–5(-7)-septata; conidia 5-septata in obscuritate 38–68 × 3.5–5 μm. Positio systematica per DNA sequentiis (a-tubulini, b-tubulini, *EF-1α,* HIS, MAT, reductasi, *URA*, *Tri101* et *PHO*) a speciebus similibus differens.

Colonies in darkness on PDA showing slow average growth rates per day of 0.8–0.9 mm at 20 °C and 1.3–1.7 mm at 25 °C. Colony color on PDA reddish-white, reddish-grey, pale red to grayish-red; reverse pigmentation reddish brown to dark brown. Colony margin entire, with brownish outline. Odor absent or moldy. Aerial mycelium on PDA less abundant, dense floccose to pannose, white, reddish-white, pale red to grayish red. Hyphae on SNA 1.5–5 μm wide. Chlamydospores and sclerotia absent. Sporulation on SNA in the dark and under black light abundant, from conidiophores formed directly on hyphae or aggregated in sporodochia on or in the agar; sporodochia formed abundantly. Conidiophores branched verticillately or unbranched, terminating with monophialides, or abbreviated as single monophialides formed on substrate hyphae. Phialides simple, subulate, ampulliform to subcylindric, monophialidic. Conidia of a single type, typically falcate and gradually curved, sometimes sigmoid or straight, dorsiventral, most frequently widest at the midregion of their length, tapering and curving toward both ends, with an arcuate apical cell and a distinct basal foot cell, upper and lower halves asymmetric,(3-)4–5(-7)-septate. In the dark, 5-septate conidia: 38–68 × 3.5–5 μm in total range, 51.1–58.6 × 4.0–4.5 μm on average, (ex-type strain: 38–51.1–68 × 3.5–4.1–5 μm). Based on analyses of DNA sequence data from seven individual loci (α-tubulin, β-tubulin, *EF-1α,* HIS, MAT, reductase, *URA*, *Tri101* and *PHO*) and the combined dataset, *F. louisianense* was strongly supported as phylogenetically distinct from other FGSC species.

HOLOTYPUS: BPI 881005, a dried culture, isolated from wheat seed, *Triticum aestivum* L., in Jefferson Davis Parish Louisiana in 2007, deposited in the herbarium of BPI (US National Fungus Collection, Beltsville, MD), USA. Ex holotype culture: NRRL 54197, CBS 127525. Other strains examined: NRRL 54196 ex wheat seed in Louisiana, USA in 2007.

Etymology: The epithet *louisianense* refers to the type locality, Louisiana in the United States of America.
Distribution: Louisiana, United States of America.

F. louisianense formed narrow conidia 4.0–4.5 μm wide on average (Figs. 2B and 3) similar to *Fusarium austroamericanum*, *Fusarium boothii*, *F. meridionale* and *Fusarium mesoamericanum*. *F. louisianense*, however, does not form conidia with a narrow apical beak in contrast to those of *F. austroamericanum*, *F. boothii* and *F. meridionale*. *F. mesoamericanum*, and some strains of *F. austroamericanum*, do not form beaked conidia. Conidia of *F. mesoamericanum* and *F. austroamericanum*, however, were typically straight and, in addition, those of *F. mesoamericanum* were most frequently widest above the mid-region. By way of contrast, conidia of *F. louisianense* were gradually curved and most frequently widest at the mid-region. Using these characters, *F. louisianense* can be distinguished morphologically from the other known species of the FGSC. In addition, the slow growth rates of *F. louisianense* on PDA (i.e., 0.8–0.9 mm at 20 °C and 1.3–1.7 mm at 25 °C) also may help differentiate *F. louisianense* phenotypically. Recognition of *F. louisianense* was strongly supported using the exclusivity criterion under GCPSR (Table 1). *F. louisianense* formed a strongly supported clade with *F. graminearum* and *F. gerlachii* in the multilocus phylogeny (Fig. 1).

Appendix B. Supplementary material

Supplementary data associated with this article can be found, in the online version, at doi:10.1016/j.fgb.2011.09.002.

References

Anderson, J., Funt, J., Thompson, D.A., Prabhu, S., Socha, A., Sirjushing, C., Dettman, J.R., Parreiras, Guttman, D.S., Regev, A., Kohn, L.M., 2010. Determinants of divergent adaptation and Dobzhansky-Muller interaction in experimental yeast-populations. Curr. Biol. 20, 1383–1388.

Aoki, T., O'Donnell, K., 1999. Morphological characterization of *Fusarium pseudograminearum* sp. nov., formerly recognized as the Group 1 population of *Fusarium graminearum*. Mycologia 91, 597–609.

Boutigny, A.-L., Ward, T.J., Van Coller, G.J., Flett, B., Lamprecht, S.C., O'Donnell, K., Viljoen, A., 2011. Analysis of the *Fusarium graminearum* species complex from wheat, barley and maize in South Africa provides evidence of species-specific differences in host preference. Fungal Genet. Biol. 48, 914–920.

Carter, J.P., Rezanoor, H.N., Desjardins, A.E., Nicholson, P., 2000. Variation in *Fusarium graminearum* isolates from Nepal associated with their host of origin. Plant Pathol. 49, 452–460.

Carter, J.P., Rezanoor, H.N., Holden, D., Desjardins, A.E., Plattner, R.D., Nicholson, P., 2002. Variation in pathogenicity associated with the genetic diversity of *Fusarium graminearum*. Eur. J. Plant Pathol. 108, 573–583.

Chandler, E.A., Simpson, D.R., Thomsett, M.A., Nicholson, P., 2003. Development of PCR assays to *Tri7* and *Tri13* trichothecene biosynthetic genes, and characterization of chemotypes of *Fusarium graminearum*, *Fusarium culmorum* and *Fusarium cerealis*. Physiol. Mol. Plant Pathol. 62, 355–367.

Cuomo, C.A., Guldener, U., Xu, J.-R., Trail, F., Turgeon, B.G., di Pietro, A., Walton, J.D., Ma, L.-J., Baker, S.E., Rep, M., Adam, G., Antoniw, J., Baldwin, T., Calvo, S., Chang, Y.-L., Decaprio, D., Gale, L.R., Gnerre, S., Goswami, R.S., Hammond-Kosack, K., Harris, L.J., Hilburn, J., Kennell, J., Kroken, S., Mannhaupt, G., Mauceli, E., Mewes, H.-W., Mitterbauer, R., Muehlbauer, G., Munsterkotter, M., Nelson, D., O'Donnell, K., Ouellet, T., Qi, W., Quesneville, H., Ronceero, M.I.G., Seong, K.-Y., Tetko, I.V., Urban, M., Waalwijk, C., Ward, T.J., Yao, J., Birren, B.W., Kistler, H.C., 2007. The genome sequence of *Fusarium graminearum* reveals localized diversity and pathogen specialization. Science 317, 1400–1402.

Desjardins, A.E., Proctor, R.H., 2010. Genetic diversity and trichothecene chemotypes of the *Fusarium graminearum* clade isolated from maize in Nepal and identification of a putative new lineage. Fungal Biol. 115, 38–48.

Dettman, J.R., Anderson, J.B., Kohn, L.M., 2010. Genome-wide investigation of reproductive isolation in experimental lineages and natural species of *Neurospora*: identifying candidate regions by microarray-based genotyping and mapping. Evolution 64, 694–709.

Dettman, J.R., Jacobson, D.J., Taylor, J.W., 2003. A multilocus genealogical approach to phylogenetic species recognition in the model eukaryote *Neurospora*. Evolution 57, 2703–2720.

Drummond, A.J., Rambaut, A., 2007. BEAST: Bayesian evolutionary inference by sampling trees. BMC Evol. Biol. 7, 214.

Edwards, S.V., Liu, L., Pearl, D.K., 2007. High resolution species trees without concatenation. Proc. Nat. Acad. Sci. USA 104, 5936–5941.

Gale, L.R., Chen, L.-F., Hernick, C.A., Takamura, K., Kistler, H.C., 2002. Population analysis of *Fusarium graminearum* from wheat fields in Eastern China. Phytopathology 92, 1315–1322.

Gale, L.R., Harrison, S.A., Ward, T.J., O'Donnell, K., Milus, E.A., Gale, S.W., Kistler, H.C., 2011. Nivalenol-type populations of *Fusarium graminearum* and *F. asiaticum* are prevalent on wheat in Southern Louisiana. Phytopathology 101, 124–134.

Gale, L.R., Ward, T.J., Balmas, V., Kistler, H.C., 2007. Population subdivision of *Fusarium graminearum* sensu stricto in the upper Midwestern United States. Phytopathology 97, 1434–1439.

Geiser, D.M., del Mar Jiménez-Gasco, M., Kang, S., Makalowska, I., Veeraraghavan, N., Ward, T.J., Zhang, N., Kuldau, G.A., O'Donnell, K., 2004. FUSARIUM-ID v.1.0: A DNA sequence database for identifying *Fusarium*. Eur. J. Plant Pathol. 110, 473–479.

Goswami, R.S., Kistler, H.C., 2004. Heading for disaster: *Fusarium graminearum* on cereal crops. Mol. Plant Pathol. 5, 515–525.
Goswami, R.S., Kistler, H.C., 2005. Pathogenicity and in planta mycotoxin accumulation among members of the *Fusarium graminearum* species complex on wheat and rice. Phytopathology 95, 1397–1404.
Heled, J., Drummond, A.J., 2010. Bayesian inference of species trees from multilocus data. Mol. Biol. Evol. 27, 570–580.
Hillis, D.H., Dixon, M.T., 1991. Ribosomal DNA: molecular evolution and phylogenetic inference. Quar. Rev. Biol. 66, 411–453.
Jansen, C., von Wettstein, D., Schäfer, W., Kogel, K.-H., Felk, A., Maier, F.J., 2005. Infection patterns in barley and wheat spikes inoculated with wild-type and trichodiene synthase gene disrupted *Fusarium graminearum*. Proc. Nat. Acad. Sci. USA 102, 16892–16897.
Ji, L., Cao, K., Wang, S., 2007. Determination of deoxynivalenol and nivalenol chemotypes of *Fusarium graminearum* from China by PCR assay. J. Phytopathol. 155, 505–512.
Karugia, G.W., Suga, H., Gale, L.R., Nakajima, T., Tomimura, K., Hyakumachi, M., 2009. Population structure of the *Fusarium graminearum* species complex from a single Japanese wheat field sampled in two consecutive years. Plant Dis. 93, 170–174.
Kimura, M., Kaneko, I., Komiyama, M., Takatsuki, A., Koshino, H., Yoneyama, K., Yamaguchi, I., 1998. Trichothecene 3-*O*-acetyltransferase protects both the producing organism and transformed yeast from related mycotoxins: cloning and characterization of *Tri101*. J. Biol. Chem. 273, 1654–1661.
Knowles, L.L., Kubatko, L.S., 2010. Estimating species trees: an introduction to concepts and models. In: Knowles, L.L., Kubatko, L.S. (Eds.), Estimating Species Trees: Practical and Theoretical Aspects. John Wiley & Sons, Inc., Hoboken, pp. 1–14.
Kubatko, L.S., Carstens, B.C., Knowles, L.L., 2009. STEM: species tree estimation using maximum likelihood for gene trees under coalescence. Bioinformatics 25, 971–973.
Lee, J., Chang, I.Y., Kim, H., Yun, S.-H., Leslie, J.F., Lee, Y.-W., 2009. Genetic diversity and fitness of *Fusarium graminearum* populations from rice in Korea. Appl. Environ. Microbiol. 75, 3289–3295.
Marthey, S., Aguileta, G., Rodolphe, F., Gendrault, A., Giraud, T., Fournier, E., Lopez-Villavicencio, M., Gautier, A., Lebrun, M.-H., Chiapello, H., 2008. FUNYBASE: a FUNgal phYlogenomic database. BMC Bioinformatics 9, 456. doi:10.1186/1471-2105-9-456.
Meng, C., Kubatko, L.S., 2010. Detecting hybrid speciation in the face of incomplete lineage sorting using gene tree incongruence: a model. Theor. Pop. Biol. 75, 35–45.
Minervini, F., Fornelli, F., Flynn, K.M., 2004. Toxicity and apoptosis induced by the mycotoxins nivalenol, deoxynivalenol and fumonisin B1 in a human erythroleukemia cell line. Toxicol. Vitro 18, 21–28.
Minin, V., Abdo, Z., Joyce, P., Sullivan, J., 2003. Performance-based selection of likelihood models for phylogeny estimation. Syst. Biol. 52, 674–683.
O'Donnell, K., Kistler, H.C., Tacke, B.K., Casper, H.H., 2000. Gene genealogies reveal global phylogeographic structure and reproductive isolation among lineages of *Fusarium graminearum*, the fungus causing wheat scab. Proc. Nat. Acad. Sci. USA 97, 7905–7910.
O'Donnell, K., Sutton, D.A., Rinaldi, M.G., Sarver, B.A.J., Balajee, S.A., Schroers, H.-J., Summerbell, R.C., Robert, V.A.R.G., Crous, P.W., Zhang, N., Aoki, T., Jung, K., Park, J., Lee, Y.-H., Kang, S., Park, B., Geiser, D.M., 2010. An internet-accessible DNA sequence database for identifying fusaria from human and animal infections. J. Clin. Microbiol. 48, 3708–3718.
O'Donnell, K., Ward, T.J., Geiser, D.M., Kistler, H.C., Aoki, T., 2004. Genealogical concordance between the mating type locus and seven other nuclear genes supports formal recognition of nine phylogenetically distinct species within the *Fusarium graminearum* clade. Fungal Genet. Biol. 41, 600–623.
O'Donnell, K., Ward, T.J., Aberra, D., Kistler, H.C., Aoki, T., Orwig, N., Kimura, M., Bjørnstad, Å., Klemsdal, S.S., 2008. Multilocus genotyping and molecular phylogenetics resolve a novel head blight pathogen within the *Fusarium graminearum* species complex from Ethiopia. Fungal Genet. Biol. 45, 1514–1522.
O'Meara, B.C., 2009. New heuristic methods for joint species delimitation and species tree inference. Syst. Biol. 59, 1–15.
Park, B., Park, J., Cheong, K.-C., Choi, J., Jung, K., Kim, D., Lee, Y.-H., Ward, T.J., O'Donnell, K., Geiser, D.M., Kang, S., 2010. Cyber infrastructure for *Fusarium*: three integrated platforms supporting strain identification, phylogenetics, comparative genomics, and knowledge sharing. Nucl. Acids Res. 39, D640–D646.
Peraica, M., Radic, B., Lucic, A., Pavolovic, M., 1999. Toxic effects of mycotoxins in humans. Bull. World Health Org. 77, 754–766.
Pestka, J.J., Smolinski, A.T., 2005. Toxic effects of mycotoxin in humans. J. Toxicol. Environ. Health Part B: Crit. Rev. 8, 39–69.
Pringle, A., Baker, D.M., Platt, J.L., Wares, J.P., Latgé, J.P., Taylor, J.W., 2005. Cryptic speciation in the cosmopolitan and clonal human pathogenic fungus *Aspergillus fumigatus*. Evolution 59, 1886–1899.
Proctor, R.H., Hohn, T.M., McCormick, S.P., 1995. Reduced virulence of *Gibberella zeae* caused by disruption of a trichothecene toxin biosynthetic gene. Mol. Plant Microbe Interact. 8, 593–601.
Qu, B., Li, H.P., Zhang, J.B., Xu, Y.B., Huang, T., Wu, A.B., Zhao, C.S., Carter, J., Nicholson, P., Liao, Y.C., 2007. Geographic distribution and genetic diversity of *Fusarium graminearum* and *F. asiaticum* on wheat spikes throughout China. Plant Pathol. 57, 15–24.
Rambaut, A., Drummond, A.J., 2007. Tracer v1.4. Available from: <http://beast.bio.ed.ac.uk/Tracer>.
Starkey, D.E., Ward, T.J., Aoki, T., Gale, L.R., Kistler, H.C., Geiser, D.M., Suga, H., Tóth, B., Varga, J., O'Donnell, K., 2007. Global molecular surveillance reveals novel *Fusarium* head blight species and trichothecene toxin diversity. Fungal Genet. Biol. 44, 1191–1204.
Suga, H., Karugia, G.W., Ward, T., Gale, L.R., Tomimura, K., Nakajima, T., Miyasaka, A., Koizumi, S., Kageyama, K., Hyakumachi, M., 2008. Molecular characterization of the *Fusarium graminearum* species complex in Japan. Phytopathology 98, 159–166.
Sullivan, J., 1996. Combining data with different distributions of among-site rate variation. Syst. Biol. 45, 375–380.
Swofford, D.L., 2002. PAUP*: phylogenetic analysis using parsimony (*and other methods). Version 4. Sinauer Associates, Sunderland, Massachusetts.
Taylor, J.W., Jacobson, D.J., Kroken, S., Kasuga, T., Geiser, D.M., Hibbett, D.S., Fisher, M.C., 2000. Phylogenetic species recognition and species concepts in Fungi. Fungal Genet. Biol. 31, 21–32.
Taylor, J.W., Turner, E., Townsend, J.P., Dettman, J.R., Jacobson, D., 2006. Eukaryotic microbes, species recognition and the geographic limits of species: examples from the kingdom Fungi. Phil. Trans. R. Soc. B 361, 1947–1963.
Tóth, B., Mesterházy, Á., Horváth, Z., Bartók, T., Varga, M., Varga, J., 2005. Genetic variability of central European isolates of the *Fusarium graminearum* species complex. Eur. J. Plant Pathol. 113, 35–45.
Ueno, Y., Nakajima, M., Sakai, K., Ishii, K., Sato, N., Shimada, N., 1973. Comparative toxicology of trichothecene mycotoxins: inhibition of protein synthesis in animal cells. J. Biochem. (Tokyo) 74, 285–296.
Ward, T.J., Bielawski, J.P., Kistler, H.C., Sullivan, E., O'Donnell, K., 2002. Ancestral polymorphism and adaptive evolution in the trichothecene mycotoxin gene, cluster of phytopathogenic Fusarium. Proc. Natl. Acad. Sci. USA 99, 9278–9283.
Ward, T.J., Clear, R.M., Rooney, A.P., O'Donnell, K., Gaba, D., Patrick, S., Starkey, D.E., Gilbert, J., Geiser, D.M., Nowicki, T.W., 2008. An adaptive evolutionary shift in Fusarium head blight pathogen populations is driving the rapid spread of more toxigenic *Fusarium graminearum* in North America. Fungal Genet. Biol. 45, 473–484.
Xu, X., Nicholson, P., 2009. Community ecology of fungal pathogens causing wheat head blight. Ann. Rev. Phytopathol. 47, 83–103.
Yang, L., van der Lee, T., Yang, X., Yu, D., Waalwijk, C., 2008. Fusarium populations on Chinese barley show a dramatic gradient in mycotoxin profiles. Phytopathology 98, 719–727.
Yli-Mattila, T., Gagkaeva, T., Ward, T.J., Aoki, T., Kistler, H.C., O'Donnell, K., 2009. A novel Asian clade within the *Fusarium graminearum* species complex includes a newly discovered cereal head blight pathogen from the Russian Far East. Mycologia 101, 841–852.
Zeller, K.A., Bowden, R.L., Leslie, J.F., 2004. Population differentiation and recombination in wheat scab populations of *Gibberella zeae* from the United States. Mol. Ecol. 13, 563–571.
Zhang, H., Zhang, Z., van der Lee, T., Chen, W.Q., Xu, J., Xu, J.S., Yang, L., Yu, D., Waalwijk, C., Feng, J., 2010. Population genetic analyses of *Fusarium asiaticum* populations from barley suggest a recent shift favoring 3ADON producers in southern China. Phytopathology 100, 328–336.
Zhang, J.-B., Li, H.-P., Dang, F.-J., Qu, B., Xu, Y.-B., Zhao, C.-S., Lia, Y.-C., 2007. Determination of the trichothecene mycotoxins chemotypes and associated geographical distribution and phylogenetic species of the *Fusarium graminearum* clade from China. Mycol. Res. 111, 967–975.
Zwickl, D.J. 2006. Genetic algorithm approaches for the phylogenetic analysis of large biological sequence datasets under the maximum likelihood criterion [Doctoral Dissertation]. The University of Texas at Austin, 115 p.